Effect of a two-dimensional potential on the rate of thermally induced escape over the potential barrier

Siyuan Han, J. Lapointe, and J. E. Lukens
Department of Physics, State University of New York at Stony Brook, Stony Brook, New York 11794
(Received 30 March 1992)

The thermally induced escape rate of a particle trapped in a two-dimensional (2D) potential well has been investigated through experiment and numerical simulations. The measurements were performed on a special type of superconducting quantum interference device (SQUID) which has 2 degrees of freedom. The energies associated with the motion perpendicular to (transverse) and along (longitudinal) the escape direction are quite different: the ratio between the transverse and longitudinal small oscillation frequencies is $\omega_t/\omega_l \sim 7$. The SQUID's parameters, which were used to determine the potential shape and energy scales were all independently determined. All data were obtained under conditions for which the 2D thermal activation (TA) model is expected to be valid. The results were found in good agreement with the theoretical prediction. The measured thermal activation energy is found to be the same as the barrier height calculated from the independently determined potential parameters. No evidence of apparent potential barrier enhancement recently reported in a similar system was found. In addition, the results of our numerical simulations suggest that the region in which the 2D thermal activation model is applicable may be extended to barriers as low as $\Delta U \sim k_B T$.

The escape rate of a particle trapped in a one-dimensional (1D) potential well via thermal activation over the potential barrier was first studied by Kramers.[1] The thermal escape rate was found to have the simple form of the Arrhenius law:

$$\Gamma = a_t \frac{\omega}{2\pi} \exp\left[-\frac{E_0}{k_B t}\right] \tag{1}$$

where ω is the small oscillation frequency at the bottom of the well, a_t is a damping dependent numerical factor of less than unity, E_0 is the activation energy, which is equal to the potential barrier ΔU, k_B is the Boltzmann constant, and T is the absolute temperature. The prediction of Eq. (1) has been verified by many experiments and numerical simulations. In particular, the measured thermal escape rate from the metastable zero voltage state to the finite voltage state of the current biased Josephson junction and the thermal transition rate between the different fluxoid states of the single junction superconducting quantum interference device (rf SQUID) agree very well with Eq. (1).[2-4] In these experiments, the sample parameters of Josephson junctions and rf SQUID's were determined via independent measurements in order to accurately compare experiment and theory. A comprehensive review on the escape rate in 1D and multidimensional system has been given by Hänggi *et al.*[5]

Brinkman[6] first generalized Kramers' calculation of escape rate from 1D to multidimensional potentials. Later, Landauer and Swanson[7] also performed a theoretical study on the effect of higher dimensionality on the thermal escape rate. They found that the escape rate through any one of the several saddle points obeys the Arrhenius law with activation energy E_0 equal to the potential barrier ΔU which is the energy of the saddle point measured relative to the bottom of the potential well. Ben-Jacob *et al.*[8] and Tesche[9] have studied the thermal escape rate in a 2D potential. The total escape rate is the sum of all the escape events in a unit time through all the saddles surrounding the well. The rate through any one of the saddle points is given by[8]

$$\Gamma = a_t \frac{\Omega_0}{2\pi} \exp\left[-\frac{E_0}{k_B T}\right] \tag{2}$$

with $E_0 = \Delta U$, where $\Omega_0 = \omega_{lw}\omega_{tw}/\omega_{ts}$ is the attempt frequency, ω_{lw} (ω_{tw}) and ω_{ls} (ω_{ts}) are the longitudinal (transverse) small oscillation frequencies at the bottom of the well and the saddle of the potential, respectively. The 2D thermal escape rate was experimentally confirmed by Naor, Tesche, and Ketchum[10] in a dc SQUID with the transverse to longitudinal frequency ratio (TLFR) $\omega_{tw}/\omega_{lw} \simeq 1$. Recently, Sharifi, Gavilano, and Van Harlingen[11,12] reported that the thermal escape rate, observed in a dc SQUID with TLFR $\simeq 7$ and $\hbar\omega_t/k_B \simeq 23$ K, was significantly suppressed, compared to Eq. (2). They suggested that their data could be explained if the activation energy E_0 were enhanced to about 2.5 times ΔU. They also suggested that the observed deviation from Eq. (2) might be related to the large transverse frequencies (ω_{ts} and ω_{tw}) involved in their experiment.[11] Here, we report measurements of the thermal escape rate in a 2D potential using a variable I_c rf SQUID [see Fig. 1(a)], which has $\hbar\omega_t/k_B \simeq 15$ K and $5 \leq \text{TLFR} \leq 9$. The activation energies E_0 derived from our data are in good agreement with Eq. (2), i.e., $E_0 = \Delta U$, where the potential barrier height ΔU was determined to a high degree of accuracy via independent measurements. We have also performed numerical simulations of the escape rate from the 2D potential well. These results are found to be in excel-

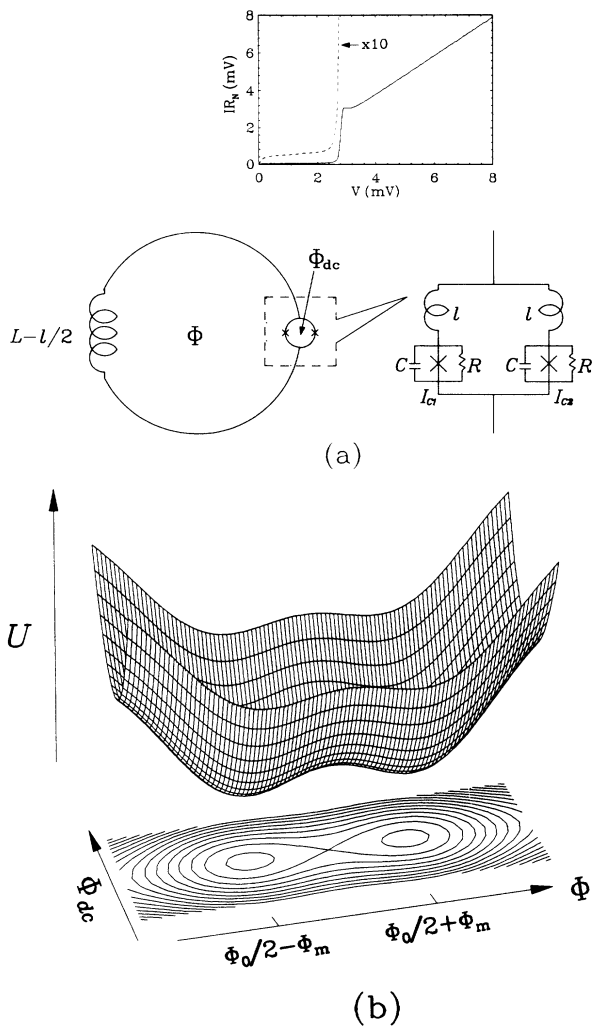

FIG. 1. (a) Schematics of a variable I_c rf SQUID. Inset: the I-V curve of a typical $Nb/Al_2O_3/Nb$ trilayer tunnel junction measured at 4.2 K with its critical current suppressed by a magnetic field. (b) Two-dimensional SQUID potential and its equal-potential contour at $\Phi_x=\frac{1}{2}\Phi_0$ and $\Phi_{xdc}=0$.

lent agreement with Eq. (2). The rest of this paper is organized as follows: in the first section the deterministic equations of motion (EOM) of a variable I_c rf SQUID, its 2D potential, and the corresponding Langevin equation in the presence of thermal fluctuation are presented. In the second section the experimental techniques and the results of the thermal escape rate measurements are described and analyzed. This is followed by a section in which the techniques employed to independently determine the sample parameters are described. In the next section the method and the results of numerical simulation are presented. In the final section the implications of our results are discussed.

I. EQUATIONS OF MOTION AND 2D POTENTIAL OF A VARIABLE I_c rf SQUID

In the variable I_c rf SQUID, the single Josephson junction in a standard rf SQUID is replaced by a small inductance, $\beta_{dc}\equiv 2\pi l I_{c0}/\Phi_0 \ll 1$, symmetric dc SQUID [Fig. 1(a)]. Here $2l$ is the loop inductance, $I_{c0}\equiv i_{c1}+I_{c2}$ is the sum of the critical currents of the two junctions, and Φ_0 is the flux quantum $h/2e$. The macroscopic dynamical variables of this system are the magnetic fluxes Φ through the rf SQUID loop and Φ_{dc} through the dc SQUID loop. Thus the system has two degrees of freedom. In the classical limit, based upon the resistively-capacitively shunted junction (RSCJ) model of Josephson junction,[13] the deterministic EOM of the variable I_c rf SQUID with two nearly identical junctions each having shunt capacitance C, shunt resistance R, and in general different critical currents I_{c1} and I_{c2} are given by[14]

$$2C\ddot{\Phi}+\frac{\dot{\Phi}}{R/2}=-\frac{\partial U(\Phi,\Phi_{dc})}{\partial\Phi}\ , \tag{3a}$$

$$\frac{C}{2}\ddot{\Phi}_{dc}+\frac{\dot{\Phi}_{dc}}{2R}=-\frac{\partial U(\Phi,\Phi_{dc})}{\partial\Phi_{dc}}\ , \tag{3b}$$

where overdot and double-overdot indicate the first- and second-order derivative with respect to time t. If the flux is expressed in units of $\Phi_0/2\pi$, then the 2D potential of the variable I_c rf SQUID is given by[14]

$$U(\varphi,\varphi_{dc})=U_0 f(\varphi,\varphi_{dc})\ , \tag{4a}$$

$$f(\varphi,\varphi_{dc})=\tfrac{1}{2}(\varphi-\varphi_x)^2+\frac{\gamma}{2}(\varphi_{dc}-\varphi_{xdc})^2 -\beta_0\cos\frac{\varphi_{dc}}{2}\cos\varphi+\delta\beta\sin\frac{\varphi_{dc}}{2}\sin\varphi\ , \tag{4b}$$

where $U_0\equiv\Phi_0^2/(4\pi^2L)$, $\gamma\equiv L/2l$ is the ratio of the inductances of the rf SQUID and the dc SQUID; φ_x (φ_{xdc}) is the externally applied flux to the rf SQUID (dc SQUID) loop, φ (φ_{dc}) is the flux enclosed in the rf SQUID (dc SQUID) loop, $\beta_0\equiv 2\pi L I_{c0}/\Phi_0$, and $\delta\beta\equiv 2\pi L(I_{c2}-I_{c1})/\Phi_0$.

The dynamical variable φ describes the in-phase motion of the two junctions which results in a current circulating in the rf SQUID loop. On the other hand, φ_{dc} describes the out-of-phase motion which results in a current circulating in the dc SQUID loop. The shape of this potential is completely determined by the dimensionless function $f(\varphi,\varphi_{dc})$ and the energy scale of the potential is determined by U_0. The two sample parameters which determine the shape of the 2D potential are β_0 and γ. For the sake of simplicity we take $\delta\beta=0$ in the remainder of this section. As we shall see below this gives an adequate description of our sample. For $\beta_0>1$, in general, the potential has metastable states. In addition, if $\gamma>\beta_0/4$, the potential has only well(s) and saddle(s) but no hill. For $\beta_0\le 1$ and $\gamma>\beta_0/4$ the potential only has one well and has no metastable state. The ratio between the transverse and longitudinal frequencies ω_t/ω_l, for a given value of φ_x and φ_{xdc}, only depends on β_0 and γ. This ratio can be modulated within some range by changing the applied flux φ_x and/or φ_{xdc}. Among all the different potential configurations one can obtain by manipulating the sample parameters and applied fluxes (Φ_x,Φ_{xdc}), a particularly interesting and important one is the symmetric double-well potential. This can be realized

by applying an external flux of $(n+\frac{1}{2})\Phi_0$, i.e., $\varphi_x=(n+\frac{1}{2})2\pi$, to the rf SQUID loop [see Fig. 1(b)]. The height of the barrier ΔU which separates the two wells can be readily adjusted by varying φ_{xdc}. This permits the rf SQUID parameters such as the barrier height of the symmetric double-well potential and the small oscillation frequencies at the bottom of the potential well to be continuously varied *in situ*.[14] In the limit of $l\to 0$, $(\gamma\to\infty)$ one has $\varphi_{dc}=\varphi_{xdc}$, so $U(\varphi,\varphi_{dc})$ goes over to the 1D potential of a rf SQUID with a single junction whose critical current is adjustable. Of course this could also be done by applying a magnetic field to a single junction. However, this approach requires either a large capacitance junction or a large field, either of which is undesirable for our purpose. The critical current of this variable I_c junction is given by $I_c=I_{c0}\cos(\varphi_{xdc}/2)$. These properties greatly enhance our ability to measure the sample's parameters accurately and to select parameters suitable for performing many different kinds of experiments such as thermal activation, macroscopic quantum tunneling, incoherent relaxation, photon-induced transition, and possibly macroscopic quantum coherence using a single sample.

By making a linear transformation of the variables from φ and φ_{dc} to $q_1=\sqrt{2}\varphi$ and $q_2=\varphi_{dc}/\sqrt{2}$, the EOM can be written as

$$C\ddot{q}_i+\frac{\dot{q}_i}{R}=-\frac{\partial U(q_1,q_2)}{\partial q_i}\ , \quad i=1,2\ . \tag{5}$$

Equations (5) are homologous to the deterministic EOM of a particle of mass C moving in a 2D potential $U(q_1,q_2)$ with damping coefficient $1/R$. One can either use Eq. (3) or Eq. (5) to describe the motion of the flux "particle." Since in our experiment the measured (controlled) quantities are fluxes φ and φ_{dc} (φ_x and φ_{xdc}), it is convenient for us to choose φ and φ_{dc} as the system's dynamical variables, Eq. (3) as the EOM, and $U(\varphi,\varphi_{dc})$ given by Eq. (4) as the potential.

In the presence of thermal fluctuation, the Langevin equations associated with the deterministic EOM are given by

$$2C\ddot{\Phi}+\frac{\dot{\Phi}}{R/2}=\frac{\Delta\Phi}{L}-I_{c0}\cos\left[\pi\frac{\Phi_{dc}}{\Phi_0}\right]\sin\left[2\pi\frac{\Phi}{\Phi_0}\right]+I_{rfn}(t)\ , \tag{6a}$$

$$\frac{C}{2}\ddot{\Phi}_{dc}+\frac{\dot{\Phi}_{dc}}{2R}=\gamma\frac{\Delta\Phi_{dc}}{L}-\frac{I_{c0}}{2}\sin\left[\pi\frac{\Phi_{dc}}{\Phi_0}\right]\cos\left[2\pi\frac{\Phi}{\Phi_0}\right]+I_{dcn}(t)\ ; \tag{6b}$$

here $\Delta\Phi\equiv\Phi_x-\Phi$ and $\Delta\Phi_{dc}\equiv\Phi_{xdc}-\Phi_{dc}$, and I_{rfn} (I_{dcn}) is the thermal noise current associated with the rf (dc) SQUID loop, which originates from the Johnson noise of junctions' shunt resistors. The noise currents are statistically independent of each other and are δ correlated. Their amplitudes are given by the fluctuation-dissipation theorem, i.e., their properties can be characterized by the following equations:

$$\langle I_{rfn}(t)\rangle=\langle I_{dcn}(t)\rangle=\langle I_{rfn}(t)I_{dcn}(t)\rangle=0\ , \tag{7a}$$

$$\langle I_{rfn}(t)I_{rfn}(t')\rangle=\frac{2k_BT}{R/2}\delta(t-t')\ , \tag{7b}$$

$$\langle I_{dcn}(t)I_{dcn}(t')\rangle=\frac{2k_BT}{2R}\delta(t-t')\ . \tag{7c}$$

To simplify the EOM, we use the following units: current in units of I_{c0}, time τ in units of ω_p^{-1}, where $\omega_p^2=2\pi I_{c0}/2C\Phi_0$ energy in units of $E_J=I_{c0}\Phi_0/2\pi$, and flux in units of $\Phi_0/2\pi$. The dimensionless damping parameter is defined as $G=(RC\omega_p)^{-1}$. The EOM are then reduced to

$$\ddot{\varphi}+G\dot{\varphi}=\frac{\Delta\varphi}{\beta_0}-\cos\frac{\varphi_{dc}}{2}\sin\varphi+i_{rf_n}(\tau)\ , \tag{8a}$$

$$\ddot{\varphi}_{dc}+G\dot{\varphi}_{dc}=\frac{4\gamma\Delta\varphi_{dc}}{\beta_0}-2\sin\frac{\varphi_{dc}}{2}\cos\varphi+4i_{dc_n}(\tau)\ , \tag{8b}$$

where the overdot and double overdot denote the first and second derivative with respect to τ, respectively. The relation between the amplitudes of the thermal noise currents is $\langle i_{rfn}^2\rangle=4\langle i_{dcn}^2\rangle$ which reflects the fact that the dissipation associated with the rf SQUID loop is four times that associated with the dc SQUID loop: the circulating current in rf SQUID loop sees the two junctions' resistances in parallel while the circulating current in dc SQUID loop sees them in series.

II. DETERMINATION OF THE SQUID PARAMETERS

Traditionally, the thermal activation energy barrier ΔU is deduced from the slope of $\ln(\Gamma)$ vs $1/k_BT$ plot because usually one lacks knowledge about the details of the potential, or the parameters which specify the potential cannot be independently determined. For a SQUID the potential is exactly known in terms of the SQUID parameters such as the loop inductance and the critical current of the junction. If one can independently measure these parameters, i.e., not determining them from the thermal escape rate measurement, the potential then can be completely determined and the effects other than potential barrier height on the thermally induced escape can be investigated.

For the SQUID potential given by Eq. (4) one can see that at any value of the external fluxes Φ_x and Φ_{xdc} a minimum of four SQUID parameters is needed to completely specify the potential's shape and energy scale. In addition, one needs to know the junction capacitance C in order to determine the small oscillation frequencies (ωs). The first four SQUID parameters mentioned above can be chosen as β_0 (or I_{c0}), $\delta\beta$ (or $I_{c2}-I_{c1}$), γ, and L (or l). The dissipation is specified by R, the shunt resistance in the RSCJ model. In Table I we list the techniques used to measure the minimum set of parameters needed to calculate the potential and the associated ωs. All the

TABLE I. The techniques used to determine the variable I_c SQUID parameters. *I-V* and SQUID resonance step measurements were made on a coprocessed sample without the rf SQUID loop. Zero-field step measurements were made on junctions fabricated with the same process.

Techniques	Parameters
Φ vs Φ_x at $\Phi_{xdc}=\Phi_0/2$	β_0, $\delta\beta$, γ
dc SQUID resonance step	lC
Zero-field step	C
Calculated from sample geometry	L,l
dc *I-V* curve	R_N

methods except the first one in Table I are commonly used in measuring Josephson junction and SQUID parameters[15–18] and will not be described extensively. The first method listed in Table I is rather unique to the variable I_c SQUID parameter determination and is discussed in detail below.

One must notice that the 2D potential $U(\Phi,\Phi_{dc})$ is periodic in both Φ and Φ_{dc} provided the external fluxes are changed by integral Φ_0, i.e.,

$$U(\Phi+n\Phi_0,\Phi_{dc}+2m\Phi_0,\Phi_x+n\Phi_0,\Phi_{xdc}+2m\Phi_0) = U(\Phi,\Phi_{dc},\Phi_0,\Phi_{xdc}) ,$$

where n and m are integers. This property of the potential makes the experimental calibration of Φ, Φ_{dc}, Φ_x, and Φ_{xdc} straightforward and very accurate. In particular, at $\Phi_{xdc}=\Phi_0/2$ (corresponding to the minimum I_L), for a SQUID such as ours having $\beta_0<6$, $\gamma>\beta_0/4$, and $\delta\beta/\beta_0<10\%$ a change in Φ_x by one flux quantum results in a precise change of one flux quantum in Φ. These constraints on the SQUID parameters ensure that the Φ vs Φ_x curve is not hysteretic. The shape of the equilibrium Φ vs Φ_x curve and thus $d\Phi/d\Phi_x$ vs Φ_x at the minimum I_c is completely determined by β_0, $\delta\beta$, and γ. $d\Phi/d\Phi_x$ as a function of Φ_x can be numerically calculated from the potential $U(\Phi,\Phi_{dc})$ using the steepest descent approximation by simultaneously solving $\partial U/\partial\Phi=0$ and $\partial U/\partial\Phi_{dc}=0$. This approximation is very good for the situation considered here. The values of β_0, $\delta\beta$, and γ used to calculate the theoretical curve were adjusted until a satisfactory fitting to the measured $d\Phi/d\Phi_x$ vs Φ_x curve was obtained. These fitting parameters were then used in all other calculations of the potentials and ωs. The $d\Phi/d\Phi_x$ vs Φ_x data, with noise reduced by signal averaging, is shown in Fig. 2 compared to the best fit. The SQUID parameters obtained from the fit are $\gamma=19.5\pm1$ pH, $\beta_0=4.10\pm0.05$, and $\delta\beta/\beta_0=(I_{c2}-I_{c1})/I_{c0}\leq4.5\%$. The fitting quality characterized by the χ^2 is very sensitive to the values of the parameters.[19] Typically, a change of 1% in β_0, 4% in γ, or 8% in $\delta\beta$ would significantly increase the χ^2, showing that this technique provides an accurate estimate of these three SQUID parameters.

To measure the thermal escape rate in a 2D potential, we have fabricated variable I_c SQUID's. The junctions were 1×1 μm^2 $Nb/Al_2O_3/Nb$ tunnel junctions of very low subgap leakage typically having a quality factor[20]

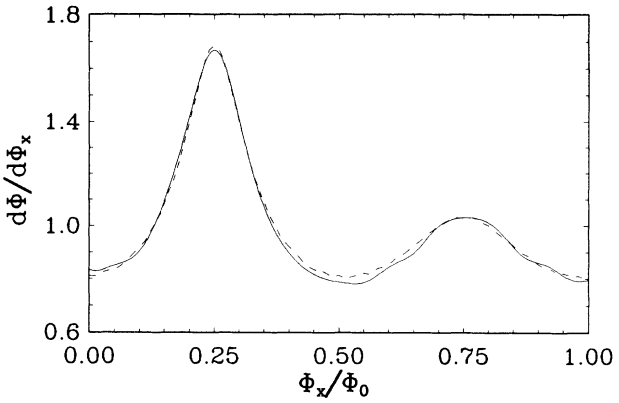

FIG. 2. $d\Phi/d\Phi_x$ vs Φ_x at $\Phi_{xdc}=\Phi_0/2$. The dashed line is calculated with $\beta_0=4.1$, $\delta\beta/\beta_0=4.5\%$, and $\gamma=19.5$. The solid line is the experimental data.

$V_m\simeq70$ mV at 4.2 K. The *I-V* curve of a current biased dc SQUID (without loop L) cofabricated with the variable I_c SQUID sample is shown in the inset of Fig. 1(a). The dc SQUID loop inductance $2l=11.8$ pH is calculated from the sample geometry. The capacitance of our 1 μm^2 $Nb/Al_2O_3/Nb$ tunnel junctions was found to be 46 ± 6 fF (including the parasitic capacitance of $\simeq5$ fF) from the resonance step in the *I-V* curve of the unshunted dc SQUID using $l=5.9$ pH. This value of specific capacitance agrees well with both the previously reported value of 40 fF/μm^2 and our zero field step measurement of 40×1.5 μm^2 junctions (where the effect of the parasitic capacitance is negligible).[21] The rf SQUID loop inductance $L=233\pm12$ pH determined from the measured values of γ and l is also in good agreement with that calculated from the sample geometry and that determined from the previous measurements of the thermal escape/MQT rate in a heavily damped single junction SQUID with similar geometry.[5] By measuring the value of Φ_x at which the system escapes from the metastable state as a function of Φ_{xdc}, taking into account the effect of thermally induced escape or of quantum tunneling, the SQUID parameter β_0 was found to be 4.1 ± 0.04 which is consistent with the value obtained through the $d\Phi/d\Phi_x$ measurement.

With the essential SQUID parameters (except R) independently determined, we can calculate the potential barrier height ΔU and all the ωs at any external fluxes Φ_x and Φ_{xdc}. This enables us to study the effect of higher dimensionality on the thermally induced escape over a potential barrier from a metastable (bistable) 2D potential well. The necessity and importance of determining the barrier height ΔU and the ωs other than from measured temperature dependence of the thermal activation rate cannot be overemphasized in this study. Without this accurate independent knowledge of ΔU and the ωs our conclusions would be very limited.

III. MEASUREMENT OF THERMAL ESCAPE RATE

The measurements of thermal escape rates from the 2D potential well were made in a highly shielded ^{4}He cryo-

stat and in a dilution refrigerator. All signals (Φ, Φ_x, and Φ_{xdc}) were inductively coupled to the sample SQUID. The leads to the room-temperature instruments were all filtered by cooled (~ 0.7 K) low pass filters. The sample SQUID was enclosed in a NbTi can. Mu metal shields and a Helmholtz coil were employed to reduce the ambient field to $\sim 2\times 10^{-7}$ T. The electronics were housed in a screen room to minimize the interference on the sample. The electrical and magnetic shielding were tested during each cooldown and were found effective. The shape and characteristics of the 2D potential, such as ΔU, ω_{lw}, ω_{tw}, ω_{ls}, and ω_{ts}, were adjusted by varying Φ_x and Φ_{xdc} to get the desired value. The amount of applied fluxes Φ_x and Φ_{xdc} can be controlled with high accuracy ($\leq 10^{-5}\Phi_0$). Thus the barrier height of the potential and all the characteristic frequencies can be determined from Eq. (4) using the independently measured values of L, C, β_0, $\delta\beta$, and γ.

As mentioned in the last section, for an applied flux $\Phi_x=(n+\frac{1}{2})\Phi_0$, where n is an integer, the potential is symmetric about $\Phi=\frac{1}{2}\Phi_0$ and has two minima at $\Phi_0/2\pm\Phi_m$ separated by a barrier ΔU [cf. Fig. 1(b)]. The barrier height $\Delta U/k_B$ can be continuously modulated *in situ* from ~ 143 K for $\Phi_{xdc}=0$ to 0 for $\Phi_{xdc}\geq 0.405\Phi_0$, for the sample studied in this work. The thermal fluctuations cause the SQUID to jump between these two energetically degenerated minima corresponding to the flux particle moving back and forth through the saddle between the left and the right potential wells. The flux Φ through the sample SQUID was monitored by a dc SQUID magnetometer which was weakly coupled to the sample. The output of the magnetometer was sent to an electronic counter or a spectrum analyzer to measure the transition rate between the two wells. At temperatures where the measurements were done ($T\geq 1.4$ K), quantum corrections to thermal activation were negligible[22,23] since the crossover temperature T_{cr} between thermal activation and macroscopic tunneling is about 0.3 K for Φ_{xdc} in the range of 0.314 to $0.329\,\Phi_0$, used for the measurements presented here.

The thermally induced transition rate given by Eq. (2) can be rewritten as

$$\ln(\Gamma/\mathrm{sec}^{-1})=A-B\frac{\Delta U}{k_BT} \tag{9}$$

with $A=\ln[a_t(\Omega_0/2\pi)/\mathrm{sec}^{-1}]$ and $B=1$. The damping factor a_t is given by $a_t=\sqrt{1+\lambda^2}-\lambda$ with $\lambda=1/(2RC\omega_{ls})$ for intermediate and heavy damping, and

$$a_t=\frac{2\pi\omega_{ts}}{\omega_{tw}\omega_{lw}RC}\frac{\Delta U}{k_BT}$$

for weakly coupled degrees of freedom (such as our sample) and low damping[5] (i.e., $RC\sqrt{\omega_{lw}\omega_{tw}}\gg\Delta U/k_BT$). We have directly measured the transition rate Γ as a function of $\Delta U/k_BT$ over the range $1<\Gamma<10^3$. This corresponds to $\Delta U/k_BT$ varying from about 19.5 to 23.5, assuming intermediate damping. The relatively small accessible range of $\Delta U/k_BT$ in our measurements is due to the limited bandwidth of the magnetometer (several kHz) used to monitor Φ. The value of $\Delta U/k_BT$ was changed either by modulating ΔU *in situ* via changing Φ_{xdc} at constant temperature or by varying temperature while keeping ΔU constant. In all the measurements the temperature was regulated to within 1 mK of the set point. Typical results of these rate measurements are shown in Fig. 3 where the logarithm of Γ is plotted as a function of $\Delta U/k_BT$. For each set of data, all the points apparently fall on a straight line which confirms that the transition rate obeys the Arrhenius law. Linear least-square fitting was then performed for each set of data to get the values of A and B [Eq. (9)]. The results are listed in Table II. The values of B obtained from our data are all within 2% equal to unity, within experimental uncertainty of about 6% as predicted by the 2D thermal activation model.[5,8]

The values of a_t, obtained from a best fit of $\ln(\Gamma/\mathrm{s}^{-1})$ vs $1/k_BT$ and the calculated $\ln(\Omega_0/2\pi)$ using independently determined potential parameters, fall between 0.37 and 5.5 due to the relatively large uncertainties associated with the fitting parameter A. Noting that, the upper limit of a_t in the thermal activation model is unity. This range of a_t is consistent with both the low damping and intermediate damping regime and corresponds to values of R from 51 Ω to 30 kΩ. At this point we cannot identify which damping regime the sample was actually in. However, our data show that the damping was not caused by the BCS subgap quasiparticle conductance, because, if this were the case, the sample would be in the low damping regime and the prefactor would be

$$e^A=\frac{\Delta U/k_BT}{R_NC}\exp(-\Delta_{\mathrm{Nb}}/k_BT)\,,$$

where Δ_{Nb} is the energy gap in niobium and is essentially temperature independent through the range of our data. This would result in an apparent increase in the activation energy by an amount of Δ_{Nb}, which is about 50% of the potential barrier ΔU, resulting in an escape rate about

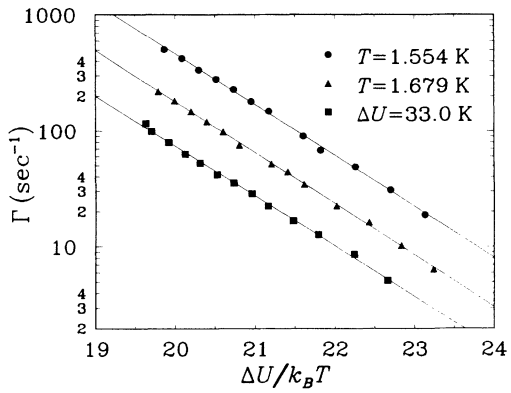

FIG. 3. Measured thermal activation rates in 2D SQUID potentials. The solid circles (RH1) and the solid triangles (RJ2): modulating ΔU at constant temperature; the solid squares (RJ1): varying temperature at constant ΔU. For clarity, the transition rates represented by the solid triangles and the solid circles are multiplied by factors 2 and 4, respectively. The solid lines are the best fit to the data. The results of the fit are listed in Table II.

TABLE II. The values of A and B obtained from the least-square fit of the measured escape rate Γ to $\ln(\Gamma/s^{-1}) = A - B(\Delta U/k_B T)$ (cf. Fig. 3) and the values of $\ln(a_t)$ determined from A and $\ln[(\Omega_0/s^{-1})/2\pi]$ which is 24.6±0.1 calculated using the independently determined potential parameters β_0, γ, L, $\delta\beta$, and C.

Data set	A	B	$\ln(a_t)$
RH1	25.0±1.2	1.01±0.07	0.4±1.3
RJ1	24.3±0.5	0.99±0.06	−0.3±0.6
RJ2	24.8±1.1	1.02±0.07	0.2±1.2

four orders of magnitude lower than the observed rate.

Using only the data on $\Gamma(T)$ for $\Delta U = \text{const}$, one might argue that our sample was in the low damping regime with a temperature dependent resistance of $R \sim R_N \exp(\Delta_{\text{Nb}}/k_B T)$ and has a *suppressed* activation energy $E_0 = \Delta U - \Delta_{\text{Nb}}$, i.e., $B < 1$. However, our data for the variation of Γ with ΔU at constant T unambiguously show that $B = 1$. This implies the damping cannot be due to the BCS subgap conductance, and more generally, exclude any sort of simple difference between E_0 and ΔU (i.e., some combination of $B \neq 1$ plus a constant offset).

IV. NUMERICAL SIMULATION

To see whether the low barrier ΔU, the large transverse frequency ω_t, or the large TLFR ω_t/ω_l could cause barrier renormalization in 2D thermal activation, we have performed numerical simulations on the system of equations (8). The algorithm adopted for our numerical simulations is a generalization to the two-dimensional potential from the one used by Büttiker, Harris, and Landauer[24] in their study of thermal activation in 1D potential. By integrating over a small time interval $\delta\tau$ and dropping the terms beyond the order of $\delta\tau^3$, Eqs. (8) are reduced to the following finite difference equations:

$$\varphi_{n+1} = 2\varphi_n - \varphi_{n-1} - G(\varphi_n - \varphi_{n-1})\delta\tau + \left[\frac{\Delta\varphi_n}{\beta_0} - \cos\frac{\varphi_{dc_n}}{2}\sin\varphi_n + \epsilon q_n\right]\delta\tau^2 , \quad (10a)$$

$$\varphi_{dc_{n+1}} = 2\varphi_{dc_n} - \varphi_{dc_{n-1}} - G(\varphi_{dc_n} - \varphi_{dc_{n-1}})\delta\tau + \left[\frac{4\gamma\Delta\varphi_{dc_n}}{\beta_0} - 2\sin\frac{\varphi_{dc_n}}{2}\cos\varphi_n + 4\epsilon p_n\right]\delta\tau^2 , \quad (10b)$$

where $\tau_n \equiv n\,\delta\tau$, $\varphi_n \equiv \varphi(\tau_n)$, $\varphi_{dcn} \equiv \varphi_{dc}(\tau_n)$, $\epsilon = \sqrt{24GK_B T/E_J}\delta\tau$, and q_n, p_n are two independent stochastic processes defined by

$$q_n = \frac{1}{\epsilon\delta\tau}\int_{\tau_{n-1}}^{\tau_n} i_{rf_n}(\tau)d\tau , \quad (11a)$$

$$p_n = \frac{1}{\epsilon\delta\tau}\int_{\tau_{n-1}}^{\tau_n} i_{dc_n}(\tau)d\tau , \quad (11b)$$

q_n and p_n have the properties of $\langle q_n\rangle = \langle p_n\rangle = \langle q_n p_n\rangle = 0$, $\langle q_n q_m\rangle = \frac{1}{12}\delta_{nm}$, and $\langle p_n p_m\rangle = \frac{1}{48}\delta_{nm}$, where δ_{nm} is the Kronecker delta. We approximate q_n and p_n by two statistically independent random numbers uniformly distributed in the interval (−0.5, 0.5) and (−0.25, 0.25), respectively.[25] The simulation was started by injecting the particle into the bottom of the 2D potential well and following its trajectory until it escaped through the saddle region and moved a certain distance away from the saddle into the other potential well. The time taken for the escape event was recorded and the particle was reinjected into the initial well to start a new process. A large number, usually 10^3, of escape events was collected for a given potential configuration and temperature. The mean escape rate for a given value of $\Delta U/k_B T$ is then obtained by averaging over all the escape events.

The range of $x \equiv \Delta U/k_B T$ covered in the simulations is $2 < x < 6$. A range of different values of β_0, γ, ω_t/ω_l, φ_x, and φ_{xdc} were used. The results of the numerical simulation are summarized in Table III and presented in Fig. 4. The parameters associated with each set of data points are also listed. In all cases, each data point is a result of averaging over $N \geq 10^3$ escape events. Note that the computing time needed for this simulation algorithm is proportional to $1/\delta\tau$ and $\exp(\Delta U/k_B T)$, respectively. The value of $\delta\tau$ was chosen such that further decreasing it does not affect the resulting average escape rate. The effect of different seeds for the random number generator was also tested. For instance, 10 sets of simulation each with a different seed and consisting of 500 escape events for a specified potential configuration gave an average lifetime with variance of less than 4%. According to Eq. (2) there should be a nearly linear relationship between $\ln(\Gamma/\omega_p)$ and $\Delta U/k_B T$:

$$\ln\left[\frac{\Gamma}{\omega_p}\right] = \ln\left[a_t\frac{\Omega_0}{2\pi\omega_p}\right] - \frac{\Delta U}{k_B T} . \quad (12)$$

In Fig. 4 we have plotted $\ln(\Gamma/\omega_p)$ vs $\Delta U/k_B T$. The solid lines were obtained by a least-square fit of the data to $\ln(\Gamma/\omega_p) = A' - B\Delta U/k_B T$. From Eq. (2) one expects that $A' = \ln(a_t\Omega_0/2\pi\omega_p)$ and $B = 1$. The value of A' and B deduced from the simulations are listed in Table III. It is clear that these results are in good agreement with the 2D thermal activation model. All the data fall on a straight line with a slope of unity (within uncertainty)

TABLE III. Numerical simulation results of the thermally activated escape from a 2D symmetric double-well potential ($\Phi_x = \frac{1}{2}\Phi_0$) with $\beta_0 = 4.0$, $L = 220$ pH, $G = 0.5$. A' and B are obtained from fitting the escape rate Γ to $\ln(\Gamma/\omega_p) = A' - B\Delta U/k_B T$ (cf. Fig. 4). The values of ω_{tw}/ω_{lw} and $\ln(a_t\Omega_0/2\pi\omega_p)$ are calculated from the potential parameters. The uncertainty is ±0.06 on A' and ±0.05 on B.

Data set	$\frac{\omega_{tw}}{\omega_{lw}}$	$\ln\left[a_t\frac{\Omega_0/\omega_p}{2\pi}\right]$	A'	B
n1	4.5	−2.09	−2.07	1.00
m1	6.2	−2.58	−2.57	1.00
r1	8.7	−2.58	−2.57	1.00
p1	12.3	−2.57	−2.56	1.00

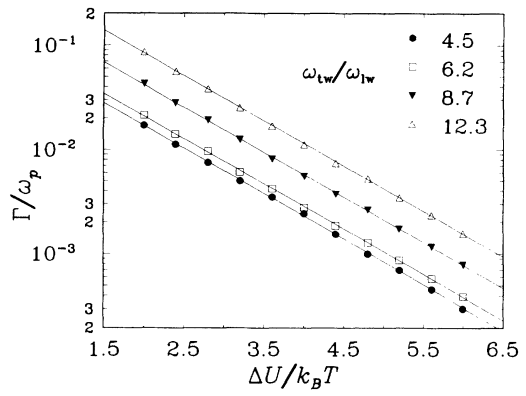

FIG. 4. Thermal activation rates in a 2D potential from our numerical simulations plotted as $\ln(\Gamma/\omega_p)$ vs $\Delta U/k_BT$. The solid lines are the best fit of the data points to Eq. (11). For clarity, the transition rates represented by the open squares (m1), the solid triangles (r1), and the open triangles (p1) are multiplied by factors 2, 4, and 8, respectively. The values of the parameters associated with the data and the fit are listed in Table III.

which indicates that the activation energy E_0 is equal to the potential barrier ΔU. The damping dependent preexponential factor $a_t\Omega_0/2\pi\omega_p$ obtained from the simulation also agrees quite well with the theory. We have not done simulations for $\Delta U/k_BT > 6$ because of the exponential increase in the required computing time. However, we feel that the range of $\Delta U/k_BT$ covered in our study is wide enough for us to claim that in a 2D potential with intermediate damping the theory gives the correct results for the escape rate via thermal activation. The study of thermal escape rates for a system having two degrees of freedom with low damping and heavy damping ($1/RC \gg \omega_{lw}, \omega_{tw}$) is underway.

V. DISCUSSIONS AND SUMMARY

We have designed and fabricated variable I_c rf SQUID's, which have two degrees of freedom, to investigate the thermally activated escape from a 2D potential well. We have introduced the equations of motion and the corresponding 2D potential of the variable I_c rf SQUID. The thermal activation rate in a 2D potential with TLFR $\simeq 7$ and $\hbar\omega_t \gg k_BT$ was measured. The SQUID's parameters that determine the shape and the energy scale of the potential have been independently determined. The measured thermal escape rates are in good agreement with the theoretical prediction of Eq. (2). The activation energies E_0 obtained from our measurements are the same, within the uncertainty of the data, as the barrier height ΔU of the *bare* potential (without enhancement or suppression). The observed dissipation modified attempt frequencies $a_t\Omega/2\pi$ are consistent with the value calculated from the 2D TA model using the independently determined SQUID's parameters. We also performed numerical simulations of thermal activation from the 2D potential wells in the region of $\sim 2 <$ TLFR $< \sim 12$ and $2 \leq \Delta U/k_BT \leq 6$. The good agreement between the simulation results and those calculated from Eq. (2) in this low to moderate barrier regime indicates that the condition $\Delta U \gg k_BT$ required by the 2D TA model might not be necessary.

These results demonstrate that there is no barrier enhancement/reduction for thermal activation in the 2D potentials having large transverse frequencies (about 15 K for the sample measured) and large value of TLFR ($\omega_t/\omega_l \sim 7$). The incomplete knowledge on the damping mechanism (i.e., R) does not affect the conclusion made above. In addition, the pre-exponential factors e^A determined from our data are consistent with the values calculated from 2D TA model with either low or intermediate damping using the measured SQUID's parameters. The good quantitative agreement between the measured thermal activation rates and those calculated from Eq. (2) confirms that when the conditions $\Delta U \gg k_BT$ and $\Delta U \gg \hbar\omega_l$ are satisfied and the damping is low or intermediate, the effect of barrier renormalization (if any) is negligible and Eq. (2) can be safely applied.

The nature of the dissipation observed in the experiment is still not yet clear (we can only say it was not due to the BCS subgap quasiparticle conductance). It is obviously impossible to directly measure the normal resistance R_N and the subgap resistance R_{qp} of the junctions in our SQUID. However, a fairly good estimate on R_N can be obtained from the junctions made using the same process and having similar critical current densities. The measured value of I_cR_N of our current biased junctions was about 2.15 mV (the effect of thermal activation on critical current was taken into account) which gives $R_N = 371\ \Omega$ for two junctions in parallel in the sample SQUID. This is within the range of 51 Ω to 30 kΩ determined from the measured thermal activation rate vs $\Delta U/k_BT$. This observed dissipation was much stronger than that expected from the subgap quasiparticle tunneling, which would correspond to $R \sim 10^7\ \Omega$ at 1.6 K. The dissipation is unlikely due to the normal resistance of the junctions but could arise from the effect of the surrounding electromagnetic environment on the sample, similar in nature to those observed by Johnson *et al.*[26] and Tinkham.[27]

In summary, the thermal escape rate from a 2D potential of a particle having two degrees of freedom has been investigated experimentally and numerically. In the experiment, the potential has values of $\Delta U/k_BT$ between about 19 to 24 and values of $\Delta U/\hbar\omega_{lw}$ between about 9 to 16. The conditions required for the validity of the thermal activation model were satisfied very well in the experiments. The measured thermal escape rate in the 2D potential agrees very well with the theory, i.e., for a two-dimensional potential the thermal activation energy E_0 is equal to the *bare* potential barrier ΔU and the main effect of the 2D potential is to renormalize the attempt frequency. All sample parameters (except damping) were independently determined to high accuracy so that all relevant potential parameters needed to make quantitative comparison with the theory are well known. The results of our numerical simulation support the validity of the 2D thermal activation model and suggest that Eq. (2)

may also be applicable to the low barrier regime. We conclude that multiple dimensionality of the potential and the large value of TLFR alone should not cause a significant deviation of the measured thermal escape rate from that calculated from the 2D thermal activation model. More theoretical and experimental studies are needed to see what the effect of strong level quantization $\Delta U/\hbar\omega_{lw} \sim 1$ on the escape rate from a 2D potential well is.

This work was supported by the U.S. Office of Naval Research.

[1]H. A. Kramers, Physica **7**, 284 (1940).

[2]T. A. Fulton and L. N. Dunkleberger, Phys. Rev. B **9**, 4760 (1974); R.F. Voss and R. A. Webb, Phys. Rev. Lett. **47**, 265 (1981).

[3]J. M. Martinis, M. H. Devoret, and John Clarke, Phys. Rev. B **35**, 4682 (1987); Michel H. Devoret, John M. Martinis, and John Clarke, Phys. Rev. Lett. **55**, 1908 (1985).

[4]J. D. Jackel, W. W. Webb, J. E. Lukens, and S. S. Pei, Phys. Rev. B **9**, 115 (1974); D. B. Schwartz, B. Sen, C. N. Archie, and J. E. Lukens, Phys. Rev. Lett. **55**, 1547 (1985); D. B. Schwartz, Ph.D. dissertation, SUNY at Stony Brook, 1986 (unpublished).

[5]Peter Hänggi, Peter Talkner, and Michal Borkovec, Rev. Mod. Phys. **62**, 252 (1990).

[6]H. C. Brinkman, Physica **22**, 149 (1956).

[7]R. Landauer and J. A. Swanson, Phys. Rev. **121**, 1668 (1961).

[8]E. Ben-Jacob, D. J. Bergman, Y. Imry, B. J. Matkowsky, and Z. Schuss, J. Appl. Phys. **54**, 6533 (1983).

[9]C. D. Tesche, J. Low Temp. Phys. **44**, 119 (1981).

[10]M. Naor, C. D. Tesche, and M.B. Ketchen, Appl. Phys. Lett. **41**, 202 (1982).

[11]F. Sharifi, J. L. Gavilano, and D. J. Van Harlingen, Phys. Rev. Lett. **61**, 742 (1988).

[12]F. Sharifi, J. L. Gavilano, and D. J. Van Harlingen, IEEE Trans. Magn. **Mag-25**, 1174 (1989).

[13]W. C. Stewart, Appl. Phys. Lett. **12**, 277 (1968).

[14]S. Han, J. Lapointe, and J. E. Lukens, Phys. Rev. Lett. **63**, 1712 (1989); Siyuan Han, J. Lapointe, and J. E. Lukens, *Single-Electron Tunneling and Mesoscopic Devices,* Springer Series in Electronics and Photonics, Vol. 31 edited by H. Koch and H. Lübbig, (1992), p. 219.

[15]D. B. Tuckerman and J. H. Magerlein, Appl. Phys. Lett. **37**, 241 (1980).

[16]J. T. Chen and D. N. Langenberg, in *Proceedings of the 13th International Conference on Low Temperature Physics, 1972,* edited by Klaus D. Timmerhaus, William John O'Sullivan and E. F. Hammel (Plenum, New York, 1974), Vol. 3, p. 289.

[17]T. A. Fulton and R. C. Dynes, Solid State Commun. **12**, 57 (1973).

[18]J. M. Jaycox and M. B. Ketchen, IEEE Trans. Magn. **17**, 400 (1981).

[19]For the definition of χ^2 see any books on probabilities, statistics, or data analysis, e.g., W. H. Press, B. P. Flannery, S. A. Teukolsky, and W. T. Vetterling, *Numerical Recipes—The Art of Scientific Computing* (Cambridge University Press, Cambridge, 1986), p. 502.

[20]A Nb SIS tunnel junction's quality factor V_m is defined as $I_c R_{2\,mV}$, where I_c is the critical current of the junction and $R_{2\,mV}$ is the resistance measured at 2 mV.

[21]S. Washburn, R. A. Webb, R. F. Voss, and S. M. Faris, Phys. Rev. Lett. **54**, 2712 (1985); A.W. Lichienberger, C. P. McClay, R. J. Mattauch, M. J. Feldman, S. K. Pan, and A. R. Kerr, IEEE Trans. Magn. **Mag-25**, 1247 (1989); Kelin Wan, Ph.D. dissertation, SUNY at Stony Brook, 1991 (unpublished).

[22]P. Riseborough, P. Hänggi, and E. Friedkin, Phys. Rev. A **32**, 489 (1985).

[23]H. Grabert, P. Olschowski, and U. Weiss, Phys. Rev. B **36**, 1931 (1987).

[24]M. Büttiker, E. P. Harris, and R. Landauer, Phys. Rev. B **28**, 1268 (1983).

[25]Random numbers from a Gaussian distribution were also used in the simulation. No statistically significant difference was found in the results of using uniform distribution or Gaussian distribution having the same standard deviation.

[26]A. T. Johnson, C. J. Lobb, and M. Tinkham, Phys. Rev. Lett. **65**, 1263 (1990).

[27]M. Tinkham, *Single Charge Tunneling* (Plenum, New York, 1992).